Water Science and Engineering 2020, 13(1): 45–56

HOSTED BY

ELSEVIER

Check for updates

Available online at www.sciencedirect.com

Water Science and Engineering

journal homepage: wse.hhu.edu.cn

Control of wind-wave power on morphological shape of salt marsh margins

Alvise Finotello [a,b,c,*], Marco Marani [c,d], Luca Carniello [c,d], Mattia Pivato [c,d], Marcella Roner [a], Laura Tommasini [a], Andrea D'alpaos [a,c]

[a] Department of Geosciences, University of Padova, Padova 35131, Italy
[b] Department of Environmental Sciences, Informatics and Statistics, University of Venice Ca' Foscari, Venice 30172, Italy
[c] Center for Lagoon Hydrodynamics and Morphodynamics, University of Padova, Padova 35131, Italy
[d] Department of Civil, Environmental and Architectural Engineering, University of Padova, Padova 35131, Italy

Received 31 July 2019; accepted 2 December 2019
Available online 26 March 2020

Abstract

Salt marshes are among the most common morphological features found in tidal landscapes and provide ecosystem services of primary ecological and economic importance. However, the continued rise in relative sea level and increasing anthropogenic pressures threaten the sustainability of these environments. The alarmingly high rates of salt marsh loss observed worldwide, mainly dictated by the lateral erosion of their margins, call for new insights into the mutual feedbacks among physical, biological, and morphological processes that take place at the critical interface between salt marshes and the adjoining tidal flats. We combined field measurements, remote sensing data, and numerical modeling to investigate the interplays between wind waves and the morphology, ecology, and planform evolution of salt marsh margins in the Venice Lagoon of Italy. Our results confirm the existence of a positive linear relationship between incoming wave power density and rates of salt marsh lateral retreat. In addition, we show that lateral erosion significantly decreases when halophytic vegetation colonizes the marsh margins, and that different erosion rates in vegetated margins are associated with different halophytes. High marsh cliffs and smooth shorelines are expected along rapidly eroding margins, whereas erosion rates are reduced in gently sloped, irregular edges facing shallow tidal flats that are typically exposed to low wind-energy conditions. By highlighting the relationships between the dynamics and functional forms of salt marsh margins, our results represent a critical step to address issues related to conservation and restoration of salt marsh ecosystems, especially in the face of changing environmental forcings.

Keywords: Salt marshes; Wind waves; Lateral erosion; Morphodynamics; Vegetation

1. Introduction

Salt marshes are widespread morphological features in coastal and estuarine tidal landscapes (Luternauer et al., 1995; Mitsch and Gosselink, 2000; Rogers and Woodroffe, 2014). Located in the upper intertidal zone, salt marshes are ecologically and economically important as they significantly contribute to coastal primary production, support high biodiversity, and provide valuable ecosystem services (Costanza et al., 1997; Barbier et al., 2011). In particular, salt marshes mediate the exchange of water, sediment, and nutrient fluxes in coastal landscapes (Larsen and Harvey, 2010; Coco et al., 2013), sequester high rates of organic carbon (Chmura et al., 2003; Kirwan and Mudd, 2012; Mueller et al., 2018; Yousefi Lalimi et al., 2018), protect coastal areas from extreme storms (Howes et al., 2010; Temmerman et al., 2013; Möller et al., 2014), host a variety of coastal biotas (Perillo et al., 2018), and display striking biogeomorphic patterns (Adam, 1990; Marani et al., 2013; van de Vijsel et al., 2019). However, the sustainability of salt marsh ecosystems is severely threatened by climate changes and increasing anthropogenic pressures (D'Alpaos et al., 2011; Ratliff et al., 2015;

* Corresponding author.
E-mail address: alvise.finotello@unipd.it (Alvise Finotello).
Peer review under responsibility of Hohai University.

https://doi.org/10.1016/j.wse.2020.03.006

FitzGerald and Hughes, 2019). As a result, extensive salt marsh areas are being lost at alarmingly increasing rates (Day et al., 2000; Delaune and Pezeshki, 2003; Gedan et al., 2009).

The ability of salt marshes to counteract changes in external forcings depends on the complex dynamic interactions between physical and biological processes acting at different spatial and temporal scales (Morris et al., 2002; Mudd et al., 2004; Marani et al., 2010). In particular, the evolution of tidal marshes in the vertical direction results from the delicate balance and feedbacks between organic and inorganic deposition, erosion, and changes in the relative sea level. For example, colonization of salt marsh platforms by halophytic vegetation enhances both organic and inorganic deposition due to increased flow resistance, reduced bottom shear stresses, capture of sediment particles by plant stems, and direct biomass accumulation (Temmerman et al., 2005; D'Alpaos et al., 2007; Mudd et al., 2010). Moreover, halophytes control soil aeration, which feeds back into vegetation zonation and the related biogeomorphic interaction typically observed in tidal marshes (Silvestri et al., 2005; Marani et al., 2006; Morris et al., 2016). These controlling biological and physical processes, which ultimately determine whether salt marshes will aggrade, persist, or drown, have been extensively studied in past decades, resulting in a rather comprehensive understanding of the problem at hand (Kirwan and Murray, 2007; Marani et al., 2010; D'Alpaos et al., 2011).

In contrast, much less attention has been devoted to the processes governing the evolution of salt marshes on the horizontal plane. Although direct wave attack is known to chiefly control lateral erosion of tidal wetlands worldwide (Schwimmer, 2001; Mariotti et al., 2010; Marani et al., 2011), the effects of wind-wave impinging against salt marsh margins have only been recently investigated in detail (Bendoni et al., 2014, 2016; Möller et al., 2014; Tommasini et al., 2019). A general consensus has now been reached, based on the fundamental work of Marani et al. (2011), which relates lateral retreat of salt marsh margins and wind-wave power on the basis of a positive linear relationship (McLoughlin et al., 2015; Leonardi et al., 2016a). However, a complete understanding of the complex, tide-modulated morphodynamic processes occurring when waves impinge on salt marsh margins is still far from being achieved (Möller et al., 1999; Tonelli et al., 2010; Schoutens et al., 2020).

Recent studies have suggested that wind-wave exposure controls marsh edge evolution only at large spatial scales, while different extrinsic (e.g., foreshore morphology) and intrinsic (e.g., soil and vegetation properties) factors govern the retreat of salt marsh edges at smaller scales (Wang et al., 2017). Furthermore, it remains unclear whether or not vegetation helps to prevent salt marsh erosion (Feagin et al., 2009), and if the morphology, ecology, and evolution of salt marsh margins are related to their morphodynamic function (e.g., if marsh margins absorbing high wave-power are most preferentially cliffed- or ramped-shaped) (Evans et al., 2019; Schoutens et al., 2020). Addressing these issues can be crucial from conservation and restoration perspectives, allowing one to assign specific morphology to marsh margins based on the morphodynamic and ecological functions they have to fulfill. This is especially critical in view of the significant efforts put in place to provide effective ecosystem-based coastal protection (Temmerman et al., 2013), as well as to conserve and restore tidal wetland ecosystems worldwide (Day et al., 2007).

In this study we addressed these issues by investigating the recent (1970 to present) evolution of salt marshes in the microtidal Venice Lagoon of Italy, which were shown to exemplify the complex interactions and feedbacks between physical, biological, and morphological processes observed for other tidal marshes found along the world's coasts (Kearney and Fagherazzi, 2016; Leonardi et al., 2016a). By means of an integrated approach, spanning direct field measurements, remote sensing analyses, and numerical modeling, we analyzed and interpreted the relationships between wind-wave impinging against salt marsh edges, and the morphology, ecology, and evolution of the edges themselves. First, we compared the wind-wave fields of the past (1970) and present configurations of the Venice Lagoon, computed by means of a two-dimensional (depth-averaged) numerical model. Then, we compared results of numerical modeling with estimates of salt marsh erosion rates derived from remotely-sensed images and available historical data, as well as with direct field measurements of the marsh edge topography and vegetation cover carried out along 83 alongshore transects located in different salt marshes in the Venice Lagoon (Fig. 1).

2. Geomorphological settings

The Venice Lagoon is a 50-km long, 10-km wide, northeast-southwest oriented brackish water body located in the northwestern Adriatic Sea, to which it is connected by the Lido, Malamocco, and Chioggia inlets (Fig. 1) (Carniello et al., 2009; D'Alpaos, 2010). Formed during the Holocene transgression (Zecchin et al., 2009; Tosi et al., 2012), the Venice Lagoon is nowadays characterized by a mean water depth of about 1.5 m, and by a semidiurnal microtidal regime with an average tidal range of about 1.0 m and peak tidal amplitudes up to 0.75 m (D'Alpaos et al., 2013). Similarly to most tidal embayments worldwide (Zhou et al., 2014; Finotello et al., 2019b, 2020), the landscape of the Venice Lagoon alternates between deeply channelized areas, unchanneled tidal flat surfaces, and vegetated intertidal salt marshes (Marani et al., 2004; Carniello et al., 2009). The latter are typically drained by intricate networks of branching and meandering tidal channels (Finotello et al., 2018; Ghinassi et al., 2018a; Cosma et al., 2019), and are colonized by different halophytes whose spatial distribution depends on feedbacks between biomass productivity and topographic elevation (Da Lio et al., 2013; Belliard et al., 2015; D'Alpaos and Marani, 2016). Salt marshes in the Venice Lagoon are characterized by a mean elevation of about 0.25 m above mean sea level (AMSL) and are colonized by a mosaic of halophytic species, among which are the following: *Spartina maritimae*, *Limonium narbonensis*, *Sarcocornia fruticosa*, *Juncus maritimus*, *Salicornia veneta*, *Puccinellia palustris*, *Inula*

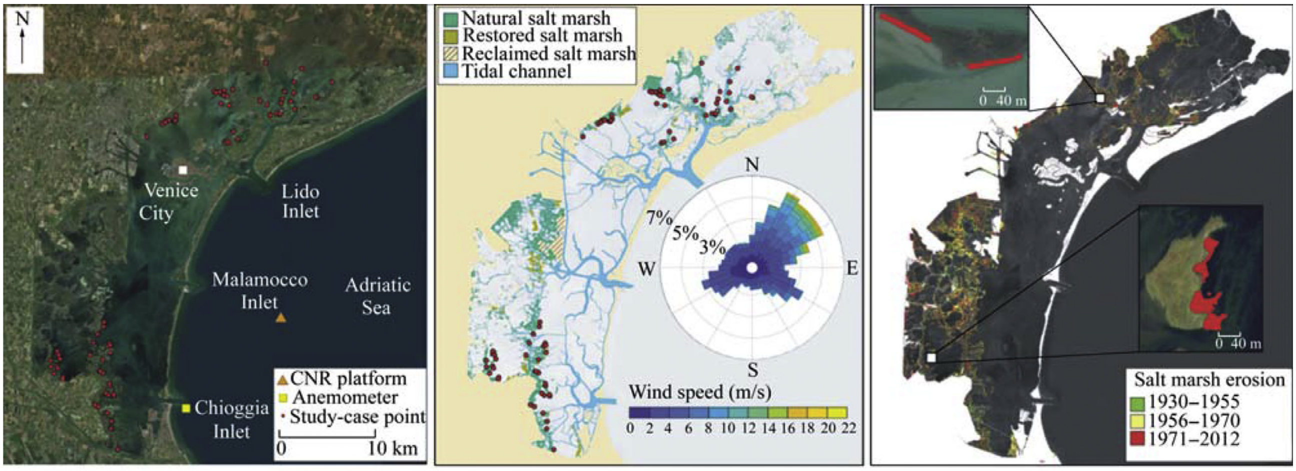

(a) Satellite 2018 Landsat image (b) Present-day salt marsh extent and wind climate (c) Erosion of salt marsh edges from 1930 to 2012

Fig. 1. Venice Lagoon (examples of regular and irregular erosion of salt marsh margins (as defined in section 3.1.2) are shown in upper and lower insets of Fig. 1(c)).

crithmoides, *Halimione portulacoides*, *Suaeda maritimae*, *Arthrocnemum macrostachyum*, and *Aster tripolium* (nomenclature follows Caniglia et al. (1997); see also Silvestri et al. (2005) and Roner et al. (2016)).

Since the 15th century, human interventions aimed at preventing the ongoing infill of the lagoon have caused significant morphological transformations (Carniello et al., 2009; Ghinassi et al., 2018b), including the dredging of navigable channels, extensive land reclamation, diversion of the major freshwater rivers, human-induced subsidence due to groundwater exploitation for industrial purposes, and, above all, the construction of jetties to stabilize the inlets, have turned the Venice Lagoon into a sediment-starved, ebb-dominated system compared to previous sediment-abundant, frictionally-dominated conditions (Gatto and Carbognin, 1981; Ferrarin et al., 2015; Finotello et al., 2019a). The combined effects of these human interventions have led to a negative sediment budget, whereby sediments exported to the open sea are more than those being imported in the lagoon (Carniello et al., 2012). This process has led to a generalized deepening of the Venice Lagoon, with a net sediment loss between 1927 and 2002 equal to 110 Mm^3. Although most of the sediments (73 Mm^3, about 70% of total loss) were lost from 1927 to 1970, mainly because of direct disposal of dredged sediment outside of the lagoon, the rate of net sediment loss through the inlets has continued to increase during the last century, from 0.3 Mm^3/year between 1927 and 1970 to 0.8 Mm^3/year from 1970 to 2002 (Sarretta et al., 2010).

In more recent times, employment of hydraulic and mechanical shellfish dredging techniques, together with waves generated by increasing motor-boat traffic, have compounded sediment export to the open sea due to (1) continual sediment resuspension from the lagoon bottom, (2) frequent destruction of the microphytobenthos film that stabilizes tidal flat surfaces, and (3) enhanced erosion of salt marsh borders (D'Alpaos et al., 2013; Chen et al., 2017; Ghinassi et al., 2019).

The ongoing erosive processes were made especially evident by the loss of salt marsh area, which was particularly pronounced during the 20th century. Starting from a surface of 180 km^2 in 1811, the area occupied by salt marshes remained approximately constant until 1901 (170 km^2) and then decreased to about 43 km^2 in the present days (Fig. 1(c)) (Carniello et al., 2009; Tommasini et al., 2019). Notably, the reduction of total salt marsh area, combined with the ongoing deepening of tidal flats, enhanced the ability of winds to generate higher waves thanks to longer fetch distances and higher water depths. This effect was particularly pronounced with respect to Bora winds, which are the prevailing winds in the Venice Lagoon, blowing from the northeast with a speed that can easily exceed 20 m/s (Fig. 1(b)) (Signell et al., 2010; Carniello et al., 2016). Increased wind-wave power further promoted marsh edge erosion due to a positive feedback mechanism that is still ongoing (D'Alpaos, 2010; Tommasini et al., 2019).

3. Methods

3.1. Characteristics and evolution of salt marsh margins

We investigated the morphological characteristics and evolution of 83 alongshore transects located at the edge of different salt marshes in the Venice Lagoon (Fig. 1(a) and (b)) by means of direct field measurement, numerical modeling, and analyses of remote sensing and available historical field data. Specifically, we computed wind-wave fields in the past (1970) and present (2012) configurations of the Venice Lagoon by means of a depth-averaged hydrodynamic wind-wave model. Then, we carried out field measurements of the height of the marsh edges and monitored vegetation cover at the study sites between the summers of 2015 and 2016. Directly measured field data and results of numerical modeling were then combined with erosion rates estimated from remotely-sensed images and available historical topographic data derived from the 1970 bathymetric survey carried out by the Venice Water Authority (Magistrato alle Acque di Venezia, “MAV” hereinafter) (Sarretta et al., 2010). The transects analyzed were about 100 m long in the alongshore direction, subject to different wind-wave exposure, and characterized by different rates and trends of lateral erosion. Our analyses focus only on naturally preserved salt marsh edges. Therefore, all the transects were located in the northern and southern portions of the lagoon, since the majority of salt marshes in the central part of the lagoon were severely affected by anthropogenic interferences such as land reclamation, protection of marsh edges against erosion, excavation of new ship canals, and extensive marsh restoration (Fig. 1(b)).

3.1.1. Salt marsh edge topography

The current height of the salt marsh edge cliff (d) was measured directly in the field in the summers of 2015 and 2016 along the study-case transects (the average value was considered in the analysis). Conversely, the 1970 cliff heights (d_0) were derived from the 1970 MAV bathymetric surveys as the difference in elevation between the marsh edge ($h_{\mathrm{m}1970}$) and the adjacent tidal flats ($h_{\mathrm{f}1970}$):

$$d_0 = h_{\mathrm{m}1970} - h_{\mathrm{f}1970} \tag{1}$$

The MAV estimated the maximum error in tidal-flat elevation to be of about ±10 cm for the 1970 bathymetry.

3.1.2. Salt marsh edge erosion

Erosion rates of the study-case margins were computed by integrating the freely available map representing the evolution of salt marsh areas between 1970 and 2002 (http://www.atlantedellalaguna.it) with marsh areas eroded from 2002 to 2012 (Fig. 1(c)). The latter were computed using georectified, high-resolution aerial photos representing the Venice Lagoon in its 2002 and 2012 configurations. The 1970−2002 marsh erosion map was produced by the MAV and is based on the same bathymetric data that were used to compute the 1970 topography of marsh edges, thus ensuring data homogeneity. Based on the eroded salt marsh area (A_{E} in m^2) and on the alongshore length of the analyzed transect (l_{t} = 100 m), we computed the linear salt marsh retreat rate (E_{L} in m/year) as follows:

$$E_{\mathrm{L}} = \frac{A_{\mathrm{E}}}{l_{\mathrm{t}}}\frac{1}{\Delta t} \tag{2}$$

where Δt (year) is the considered time interval. Subsequently, the volumetric erosion rate per unit length of marsh margins (E_{V} in m^2/year) was computed by considering the average between the past (d_0, from the 1970 survey) and the present (d) heights of the marsh cliff:

$$E_{\mathrm{V}} = \frac{(d_0 + d)E_{\mathrm{L}}}{2} \tag{3}$$

In addition, we categorized the study salt marsh margins according to the observed erosion trend. Specifically, margins that retreated almost uniformly along the analyzed transects were classified as regular, whereas marsh edges where erosion rates varied significantly along the transects, forming gullies and/or leaving behind isolated vegetation patches, were classified as irregular (Fig. 1(c)).

3.1.3. Salt marsh edge vegetation

Vegetation cover along the study transects was directly monitored in the field during the 2015 and 2016 summers, near the end of the growing season, using the square-meter quadrats technique (Bonham, 1989; Carlisle et al., 2006). Four 1 m × 1 m quadrats were randomly positioned along the analyzed 100-m alongshore transects, and species composition and percent cover were estimated from high-resolution photographs taken within each quadrat using a 225-node grid (Roner et al., 2016). A maximum of three different dominant species was then identified for each individual transect, including bare soil observed along vegetated margins wherein vegetation dieback occurred. No edges completely devoid of vegetation were found. In order to filter out possible seasonal and annual changes in vegetation cover associated with different dominant species, the collected data were finally compared with other vegetation cover data available in the literature for the same study sites (Belluco et al., 2006; Cazzin et al., 2009; Mion et al., 2010), and showed strong agreement.

3.2. Numerical modeling of hydrodynamics and wind-wave fields

A two-dimensional (depth-averaged) coupled hydrodynamic and wind-wave model (WWTM) was employed to reproduce tide propagation and wind-wave generation in shallow water environments (Defina, 2000; Carniello et al., 2005, 2011, 2012). Using a semi-implicit staggered finite element method based on Galerkin's approach, the model solves the depth-averaged shallow water equations, suitably modified in order to account for the wetting and drying processes that systematically occur in very shallow and irregular tidal domains (see Defina (2000) and D'Alpaos and Defina (2007) for a detailed descriptions of the governing equations and of the numerical scheme). The hydrodynamic module provides the wind-wave module with the flow field characteristics needed to describe the processes affecting the generation and propagation of wind waves. The wind-wave module is based on the solution of the wave-action conservation equation, parametrized using the zero-order moment of the wave action spectrum in the frequency domain (Carniello et al., 2005, 2011, 2012). The spatial and temporal distribution of the wave period is determined through an empirical function relating the peak wave period to the local wind speed and water depth (Young and Verhagen, 1996; Breugem and Holthuijsen, 2006). The model has been widely tested by comparing numerical results to hydrodynamic, wind-wave, and sediment transport data collected not only in the Venice Lagoon (Carniello et al., 2005, 2011; D'Alpaos and Defina, 2007; Mel et al., 2019), but also in other tidal embayments worldwide (Mariotti et al., 2010; Zarzuelo et al., 2015, 2018). The reader is referred to Carniello et al. (2005, 2011, 2012) for a detailed description and further information about the model calibration.

We used two existing, previously tested and accurately calibrated models reproducing the whole Venice Lagoon in its 1970 and present (2012) configurations (Tommasini et al., 2019). The computational grid representing the 1970 lagoon configuration is based on topographic surveys carried out by the MAV, which were also employed to compute the elevation of salt marsh margins and tidal flat surfaces. Conversely, the computational grid reproducing the present-day (2012) configuration of the Venice Lagoon was derived from the 2003 MAV bathymetric survey, updated by including the most recent modifications of the inlets' morphology due to the installation of mobile gates to prevent the flooding of Venice City (Mo.S.E. project).

In order to account for the modifications in the hydrodynamic and wind-wave fields that occurred during the study period, we carried out one-year-long simulations including a portion of the Adriatic Sea in front of the Venice Lagoon, where boundary conditions were imposed. Both the grids were forced using tidal levels, as well as wind velocities and directions, recorded throughout the entire year 2005 at the Consiglio Nazionale delle Ricerche (CNR) "Acqua Alta" Oceanographic Platform and at the Chioggia anemometric station (Fig. 1(a)). We selected the year 2005 because it embodied a probability distribution of wind velocities that made it representative of the typical wind wave fields observed within the Venice Lagoon over much longer periods (D'Alpaos et al., 2013; Carniello et al., 2016). Following the approach proposed by Tommasini et al. (2019), we computed, for each element of the computational grid, the mean wave power density by averaging wave power density (P_{w}) over the time-length of the whole simulation. The wave power density per unit length of wavefront was computed as follows:

$$P_{\mathrm{w}} = H^2 \rho g c_{\mathrm{g}} / 8 \tag{4}$$

where g is the gravitational acceleration; ρ is the water density; and H and c_{g} are the significant wave height and wave group celerity, respectively (see also Mariotti et al. (2010) and Marani et al. (2011)). The mean wave power densities computed for the 1970 and 2012 configurations were then linearly interpolated in order to obtain the mean wave power density ($\overline{P}_{\mathrm{w}}$) at the middle of the considered time interval (i.e., 1991). The computed $\overline{P}_{\mathrm{w}}$ was then compared with volumetric erosion rates, vegetation, and morphologic data of salt marsh margins in order to unravel the mutual interaction between incoming wave power and marsh edge morphology.

4. Results and discussion

Results of numerical modeling show a generalized increase of the mean wave power density from 1970 to 2012, which was particularly pronounced in the central part of the Venice Lagoon (Figs. 2 and 3). This finding is in agreement with previous observations (Carniello et al., 2009; Tommasini et al., 2019), and depends on a positive feedback mechanism between deepening of the lagoonal bottom, loss of salt marsh areas, and enhanced wind-wave power, given that the trend in external wave forcing over the study period was insignificant. Specifically, large erosion processes of tidal flats and subtidal platforms were initially triggered by the construction of the jetties at the inlets between 1872 and 1934, and by the excavation of the Malamocco-Marghera navigable channel in the central part of the lagoon in 1969. These interventions strongly

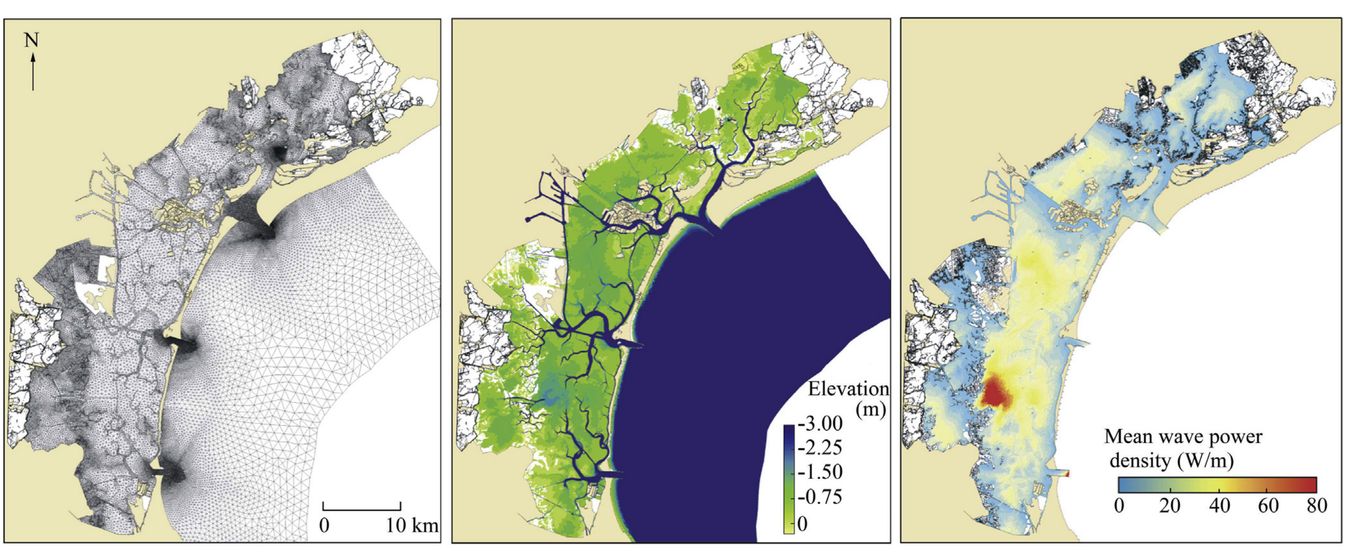

(a) Computational grid (b) Color-coded bathymetry (c) Annual mean wave power density

Fig. 2. Computational grids and results of numerical modeling for 1970.

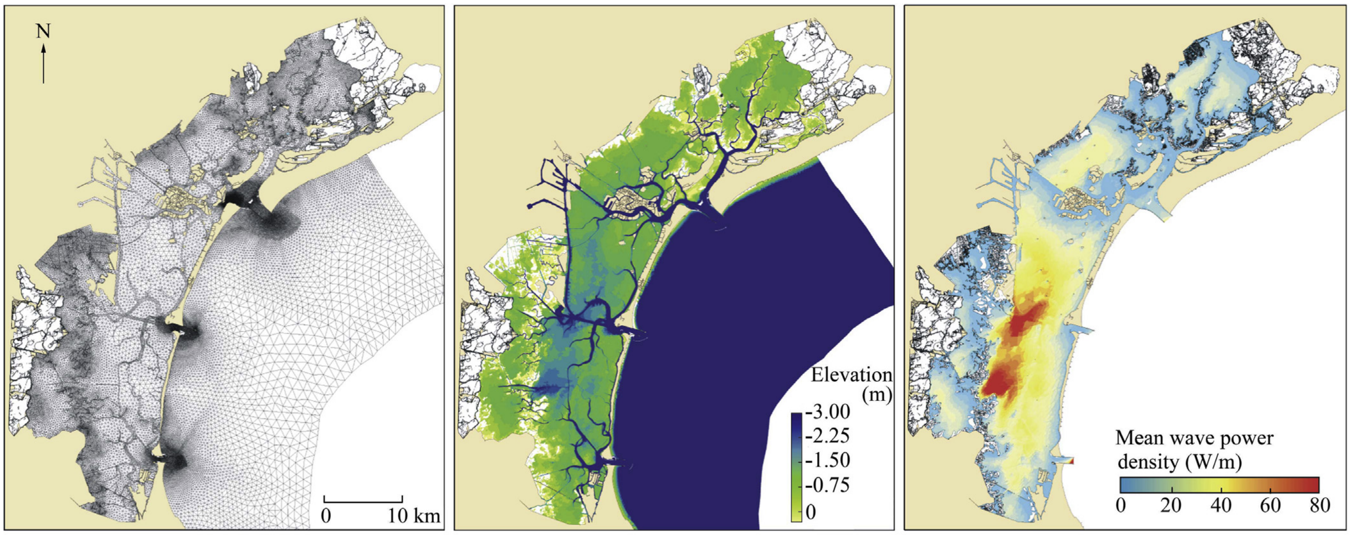

(a) Computational grid (b) Color-coded bathymetry (c) Annual mean wave power density

Fig. 3. Computational grids and results of numerical modeling for 2012.

modified the lagoon hydrodynamics and promoted net sediment loss on the order of 0.8×10^6 m^3/year between 1970 and 2002 (Sarretta et al., 2010; Carniello et al., 2012). During the same period, increasing relative sea levels caused further deepening of the lagoon, thus contributing to the increase of wave height and wave power. This ultimately resulted in extensive erosion of tidal-flat bottoms and salt marsh areas, which in turn enhanced the ability of winds to generate higher waves thanks to longer fetch distances and higher water depths (Carniello et al., 2009; Tommasini et al., 2019).

The computed mean wave power density ($\overline{P}_\mathrm{w}$) correlates with volumetric erosion rates (E_V) observed in our study sites (coefficient of determination $R^2 = 0.96$, probability value for F-test on the regression model $p < 0.001$; Fig. 4). Therefore, our data confirm the existence of a linear relationship between $\overline{P}_\mathrm{w}$ and E_V, that was established on purely theoretical grounds by Marani et al. (2011) and then empirically verified by a number of observations from different salt marshes worldwide (Leonardi et al., 2016a, 2016b). This points to a strong, first-order control exerted by incoming wind waves on the long-term evolution of salt marsh landscapes (see also Tommasini et al. (2019)). Notably, comparisons with published data show that our results fall within the range of variability typically observed for salt marshes in the Venice Lagoon (Marani et al., 2011; Tommasini et al., 2019), as well as in other tidal environments worldwide (Mariotti et al., 2010; Leonardi et al., 2016a, 2016b), and highlight the independence of $E_\mathrm{V}/\overline{P}_\mathrm{w}$ from the ratio of marsh cliff height (d) to tidal-flat bottom depth (h_f) (Fig. 5(a)), thus supporting the proportionality $E_\mathrm{V} \propto \overline{P}_\mathrm{w}$ (see Marani et al. (2011) for further details). Nonetheless, both d and h_f exhibit a statistically significant positive correlation with the observed volumetric erosion rates (Fig. 5(b) and (c)). These results point to a critical control on the erosion of the marsh boundary exerted by both the topography of the boundary itself and the bathymetry of the adjacent tidal flats. If, on the one hand, a deeper tidal-flat bottom is known to favor the generation of higher waves, which ultimately promote stronger erosion of the salt marsh margin, on the other hand the observed increase in E_V when edge cliffs are higher suggests that the lateral stability of salt marshes is enhanced by ramped margins relative to cliffed margins (Allen, 1993; Evans et al., 2019), possibly providing a valuable insight from restoration perspectives (Broome et al., 1988; Warren et al., 2002; Deheyn and Shaffer, 2007). Although previous researchers have suggested that the formation of a cliffed margin is not necessarily related to quickly retreating marshes (Pye and French, 1993), our results support the idea that lateral marsh erosion caused by wave attack mainly occurs in salt

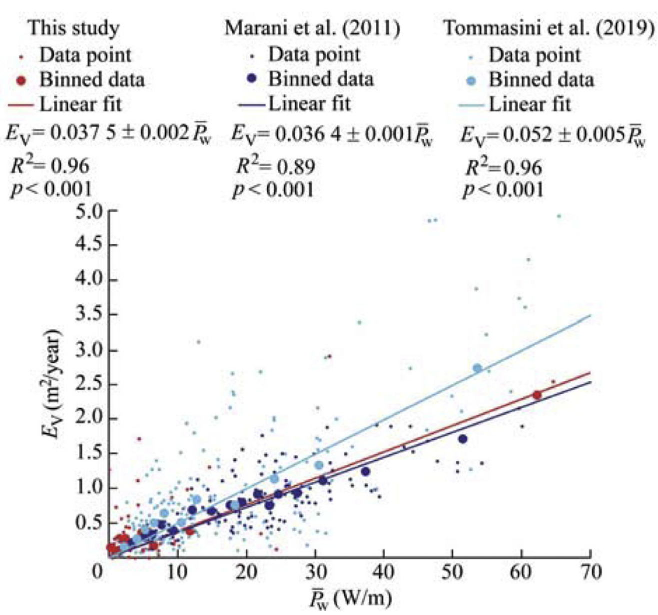

Fig. 4. Relationship between volumetric erosion rate and mean wave power density (with slope coefficients of linear regressions calculated by a standard bootstrap resampling method).

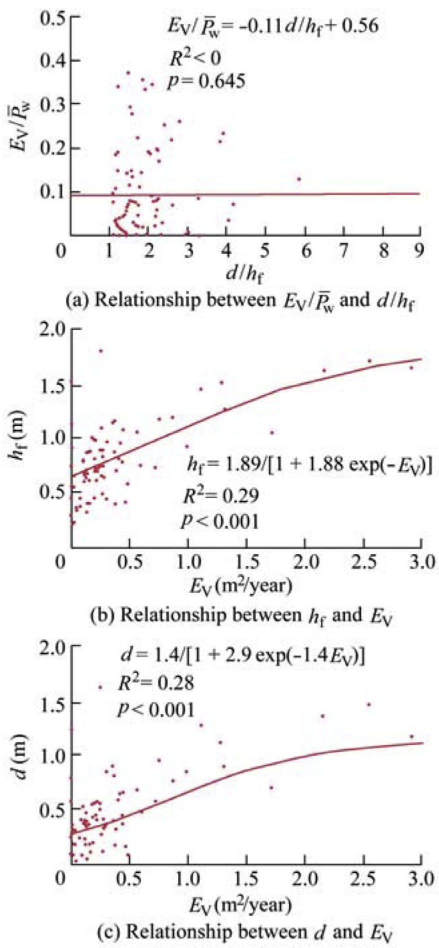

Fig. 5. Relationships between mean wave power density ($\overline{P}_w$), salt marsh cliff height (d), tidal flat depth (h_f), and volumetric erosion rate (E_V) of salt marsh edges.

marshes characterized by high scarps and surrounded by deep tidal flats.

These insights are further supported by the analyses of the erosive trends observed along the study transects (Fig. 6, in which scatter points represent outlier data) where regular (i.e., uniform) erosion occurs along margins exposed to higher wave energy, thereby promoting more pronounced volumetric erosion rates (Fig. 6(a)). A two-sample Kolmogorov-Smirnov (KS) test confirms that the observed differences are statistically significant at the $\alpha = 5\%$ significance level ($p = 0.0055$). Conversely, no significant difference is observed, in terms of incoming mean wave power, between smooth and irregular marsh margins (Fig. 6(b); $p = 0.2$ for KS test at $\alpha = 5\%$). Our results also show that high marsh cliffs are expected along smooth margins, whereas more jagged boundaries are typically more gently sloped (Fig. 6(c); $p = 0.0089$ for KS test at $\alpha = 5\%$) (Schwimmer, 2001; Priestas and Fagherazzi, 2011). These trends are consistent with empirical and numerical pieces of evidence from Leonardi and Fagherazzi (2014) and Leonardi et al. (2016b). Previous suggestions that the morphological changes of salt marsh boundaries can be used to evaluate salt marsh degradation and infer changes in wave climate (Leonardi and Fagherazzi, 2014; Leonardi et al., 2016b) support the need to accurately design marsh restoration schemes in order to account for the mutual interactions between wave exposure and the combined marsh-edge/tidal-flat morphology in determining the planform evolution of salt marshes.

In addition to wave exposure and marsh topography, different vegetation species found along the marsh edge likely represent another critical factor controlling salt marsh lateral retreat. In particular, vegetation is thought to increase the mechanical properties of the soil by binding it with live roots, thus reducing wind-wave induced erosion along the marsh edges (Feagin et al., 2008; Shepard et al., 2011; Rupprecht et al., 2017). However, previous researchers have challenged this paradigm and suggested that salt marsh vegetation does not directly act to prevent erosion of wetland edges (Kerr and Baird, 2007; Feagin et al., 2009), which should, in turn, be primarily controlled by soil type.

Our analyses show that different halophytic species are found along salt marsh boundaries characterized by different elevations (Fig. 7(a), in which scatter points represent outlier data).

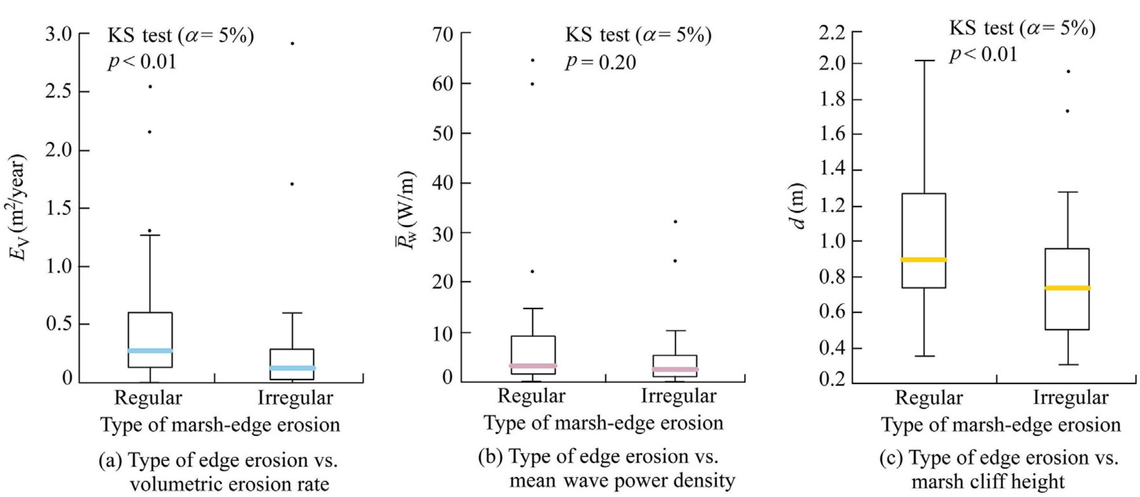

Fig. 6. Effects of erosion rate, mean wave power density, and height of marsh-edge cliff on mode of salt marsh edge retreat (as defined in section 3.1.2), and results of two-sample KS test.

The latter is known to drive vegetation zonation in tidal wetlands by controlling physical and biological processes such as salinity, soil aeration, and organic and inorganic sedimentation, which

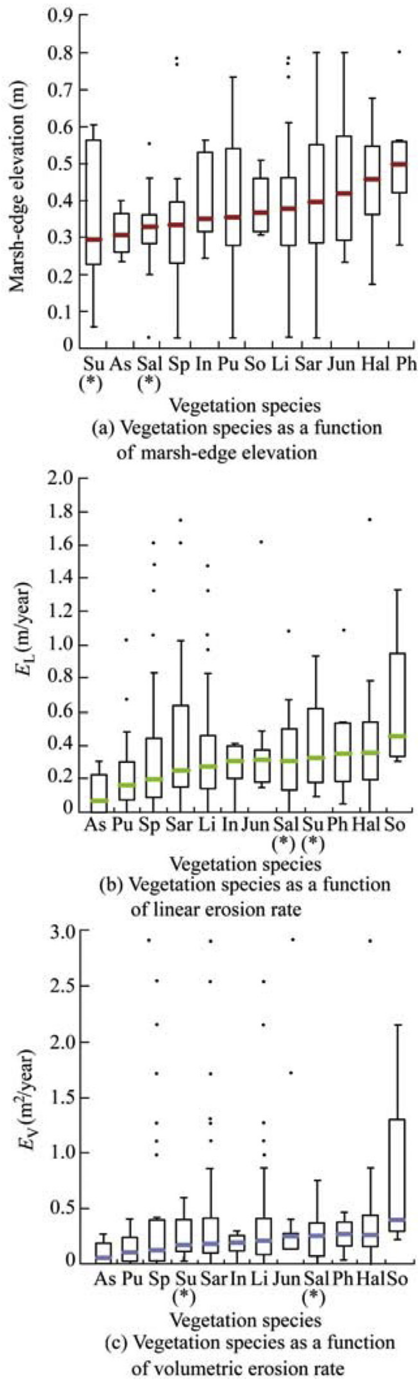

Fig. 7. Distribution of observed dominant halophytic vegetation species (“Su” indicates *Suaeda maritimae*, “As” indicates *Aster tripolium*, “Sal” indicates *Salicornia veneta*, “Sp” indicates *Spartina maritimae*, “In” indicates *Inula crithmoides*, “Pu” indicates *Puccinellia palustris*, “So” indicates bare soil, “Li” indicates *Limonium narbonensis*, “Sar” indicates *Sarcocornia fruticosa*, “Jun” indicates *Juncus maritimus*, “Hal” indicates *Halimione portulacoides*, “Ph” indicates *Phragmites australis*, and “(*)” denotes annual species).

feed back into ecomorphodynamics (Marani et al., 2013; D'Alpaos and Marani, 2016; Xin et al., 2017). The observed vegetation zonation of the marsh boundaries is consistent with previous field studies (Silvestri et al., 2005; Belluco et al., 2006; Roner et al., 2016), showing that lower marsh edges are dominated by *Suaeda maritimae*, *Spartina maritimae*, *Aster tripolium*, and *Salicornia veneta* (Fig. 7(a)). As the elevation of the marsh margin increases, *Limonium narbonensis*, *Puccinellia palustris*, *Inula crithmoides*, and *Sarcocornia fruticosa* become more common, together with unvegetated soil, while much higher salt marsh edges are characterized by the presence of *Halimione portulacoides*, *Juncus maritimus*, and *Phragmites australis*, which are less tolerant to prolonged flooding and high soil salinities (Fig. 7(a)).

Notably, our results highlight reduced salt marsh retreat, both in terms of linear and volumetric erosion rates, along vegetated marsh edges compared to margins where bare soil is one of the three dominant vegetation classes (Figs. 7(b) and 6(c)). This suggests that vegetation actively contributes to preventing erosion of salt marsh edges due to wave action. Salt marsh boundaries dominated by annual species, namely *Salicornia veneta* and *Suaeda maritimae*, show linear and volumetric erosion rates more similar to edges where bare soil is dominant (Fig. 7(b) and (c)). High erosion rates are also observed in transects dominated by *Phragmites australis*, *Halimione portulacoide*, and *Juncus maritimus*, all of which tend to colonize high-elevated marshes (Fig. 7(a)). Among the halophytes occupying less elevated marsh edges, reduced erosion rates are associated only with the presence of *Aster tripolium*, while *Suaeda maritimae* and *Salicornia veneta* exhibit erosion rates comparable with those characterizing species found in high-elevated marshes (i.e., *Phragmites australis*, *Halimione portulacoide*, and *Juncus maritimus*) (Fig. 7(b) and (c)). This is likely due to the fact that both *Suaeda maritimae* and *Salicornia veneta* are annual species, which play an important role in the pioneer colonization of unvegetated tidal flat areas, but cannot ensure significant structural stability to the soil. Conversely, root systems of perennial species that occupy low-to-middle elevated marsh areas, such as *Limonium narbonensis*, *Puccinellia palustris*, *Sarcocornia fruticosa*, and *Spartina maritimae*, are known to enhance the mechanical properties of the marsh soil, ensuring enhanced resistance to disaggregating processes such as those due to the action of waves (Cazzin et al., 2009).

Whether the observed elevation of the marsh edge and the colonizing vegetation species are in equilibrium with current external forcings, or are inherited from previously eroded marsh margins which became exposed to wave action, is still an open question. In particular, when the marsh edge retreats, the inner portion of the marsh becomes exposed to wave action. While the latter can surely cause more erosion, it can also enhance the delivery of inorganic sediment over the newly exposed marsh edges, thus increasing their elevation and promoting changes in vegetation cover. Two examples can help to exemplify this point. First, the encroachment of new vegetation species can occur when the material deposited in front of the margin as a result of erosive processes is not later reworked and removed by the action of waves and/or tides. This case is especially relevant when the elevation gradients are mild, i.e., for ramped and weakly cliffed margins, where a small increase in bottom elevations can critically result in the encroachment of new colonizing vegetation species. Second, wind waves can increase the elevation of the marsh edge by delivering organic and inorganic sediments that are deposited over the margin, by means of a spillover mechanism similar to that typically observed along the bank of tidal channels. The importance of these mechanisms in counteracting the ongoing erosion of the marsh edges is, of course, dependent on both the topographic relief they are able to establish and the possibly available window of opportunity for vegetation establishment (Hu et al., 2015; Schoutens et al., 2020), but cannot be disregarded *a priori*.

Monitoring of marsh-edge evolution and vegetation cover should be repeated periodically and extended over multiannual periods, in order to verify the possible existence of the positive feedback mechanisms suggested above and to achieve a better understanding of the processes governing the lateral evolution of salt marsh platforms.

5. Conclusions

By means of an integrated approach combining field measurements, remote sensing, numerical modeling, and analysis of historical data, we have analyzed and interpreted the relationship between wind waves and the ecomorphodynamic evolution of salt marsh margins in the Venice Lagoon. The results presented in this study suggest that, even though wind waves exert a primary control on the long-term lateral retreat, rates of salt marsh lateral erosion tend to be reduced in ramped, gently-sloped margins that (1) face shallow tidal flats, (2) are characterized by jagged planform shapes, and (3) are located in the mid-low portions of the upper intertidal zone where the establishment of soil-stabilizing halophytes is favored. Therefore, our analyses clearly indicate that the presence of vegetation is a key factor governing marsh retreat rates, and support early claims that salt marsh vegetation (1) effectively acts to reduce wave-induced lateral erosion, and (2) can possibly be used to improve the effectiveness of conservation and restoration projects by designing marsh elevations to favor encroachment of edge-stabilizing species (e.g., Donnelly and Bertness, 2001; Wang et al., 2017). Even though more analyses are required in order to better understand the long-term ecomorphological adaptation of salt marsh margins to the incoming waves, our empirical observations might provide valuable guidelines to better design effective, durable, ecosystem-based salt marsh restoration schemes.

Acknowledgements

Scientific activities were performed with the contribution of the Provveditorato for the Public Works of Veneto, Trentino Alto Adige and Friuli Venezia Giulia, provided through the concessionary of the State Consorzio Venezia Nuova and coordinated by the Consorzio per il Coordinamento delle Ricerche Inerenti al Sistema Lagunare di Venezia (CORILA).

References

Adam, P., 1990. Salt Marsh Ecology. Cambridge University Press, New York.

Allen, J.R.L., 1993. Muddy alluvial coasts of Britain: Field criteria for shoreline position and movement in the recent past. Proc. Geol. Assoc. 104(4), 241–262. https://doi.org/10.1016/S0016-7878(08)80044-2.

Barbier, E.B., Hacker, S.D., Kennedy, C., Koch, E.W., Stier, A.C., Silliman, B.R., 2011. The value of estuarine and coastal ecosystem services. Ecol. Monogr. 81(2), 169–193. https://doi.org/10.1890/10-1510.1.

Belliard, J.-P., Toffolon, M., Carniello, L., D'Alpaos, A., 2015. An ecogeomorphic model of tidal channel initiation and elaboration in progressive marsh accretional contexts. J. Geophys. Res.: Earth Surf. 120(6), 1040–1064. https://doi.org/10.1002/2015JF003445.

Belluco, E., Camuffo, M., Ferrari, S., Modenese, L., Silvestri, S., Marani, A., Marani, M., 2006. Mapping salt-marsh vegetation by multispectral and hyperspectral remote sensing. Remote Sens. Environ. 105(1), 54–67. https://doi.org/10.1016/j.rse.2006.06.006.

Bendoni, M., Francalanci, S., Cappietti, L., Solari, L., 2014. On salt marshes retreat: Experiments and modeling toppling failures induced by wind waves. J. Geophys. Res.: Earth Surf. 119(3), 603–620. https://doi.org/10.1002/2013JF002967.

Bendoni, M., Mel, R., Lanzoni, S., Francalanci, S., Oumeraci, H., Solari, L., 2016. Insights into lateral marsh retreat mechanism through localized field measurements. Water Resour. Res. 52(2), 1446–1464. https://doi.org/10.1002/2015WR017966.

Bonham, C.D., 1989. Measurements for Terrestrial Vegetation. John Wiley & Sons, New York.

Breugem, W.A., Holthuijsen, L.H., 2006. Generalized shallow water wave growth from Lake George. J. Waterw. Port, Coast. Ocean Eng. 133(3), 173–182. https://doi.org/10.1061/(ASCE)0733-950X(2007)133:3(173).

Broome, S.W., Seneca, E.D., Woodhouse, W.W., 1988. Tidal salt marsh restoration. Aquat. Bot. 32(1–2), 1–22. https://doi.org/10.1016/0304-3770(88)90085-X.

Caniglia, G., Contin, G., Fusco, M., Anoè, A., Zanaboni, A., 1997. Confronto su base vegetazionale tra due barene della laguna di Venezia. Fitosociologia 34, 111–119 (in Italian).

Carlisle, B., Carullo, M., Smith, J., Wigand, C., McKinney, R., Charpentier, M., Fillis, D., Stolt, M., 2006. Rapid Method for Assessing Estuarine (Salt) Marshes in New England, Version 1.4. Patuxent Wildlife Research Center, Laurel.

Carniello, L., Defina, A., Fagherazzi, S., D'Alpaos, L., 2005. A combined wind wave-tidal model for the Venice Lagoon, Italy. J. Geophys. Res.: Earth Surf. 110, 1–15. https://doi.org/10.1029/2004JF000232.

Carniello, L., Defina, A., D'Alpaos, L., 2009. Morphological evolution of the Venice Lagoon: Evidence from the past and trend for the future. J. Geophys. Res.: Earth Surf. 114(F4), 1–10. https://doi.org/10.1029/2008JF001157.

Carniello, L., D'Alpaos, A., Defina, A., 2011. Modeling wind waves and tidal flows in shallow micro-tidal basins. Estuar. Coast. Shelf Sci. 92(2), 263–276. https://doi.org/10.1016/j.ecss.2011.01.001.

Carniello, L., Defina, A., D'Alpaos, L., 2012. Modeling sand-mud transport induced by tidal currents and wind waves in shallow microtidal basins: Application to the Venice Lagoon (Italy). Estuar. Coast. Shelf Sci. 102–103, 105–115. https://doi.org/10.1016/j.ecss.2012.03.016.

Carniello, L., D'Alpaos, A., Botter, G., Rinaldo, A., 2016. Statistical characterization of spatio-temporal sediment dynamics in the Venice Lagoon. J. Geophys. Res.: Earth Surf. 121(5), 1049–1064. https://doi.org/10.1002/2015JF003793.

Cazzin, M., Ghirelli, L., Mion, D., Scarton, F., 2009. Completamento della cartografia della vegetazione e degli habitat laguna di Venezia: Anni 2005–2007. Lavori Soc. Ven. Sci. Nat. 34, 81–89 (in Italian).

Chen, X.D., Zhang, C.K., Paterson, D.M., Thompson, C.E.L., Townend, I.H., Gong, Z., Zhou, Z., 2017. Hindered erosion: The biological mediation of noncohesive sediment behavior. Water Resour. Res. 53(6), 4787–4801. https://doi.org/10.1002/2016WR020105.

Chmura, G.L., Anisfeld, S.C., Cahoon, D.R., Lynch, J.C., 2003. Global carbon sequestration in tidal, saline wetland soils. Global Biogeochem. Cycles 17(4), 1111. https://doi.org/10.1029/2002gb001917.

Coco, G., Zhou, Z., van Maanen, B., Olabarrieta, M., Tinoco, R., Townend, I.H., 2013. Morphodynamics of tidal networks: Advances and challenges. Mar. Geol. 346, 1–16. https://doi.org/10.1016/j.margeo.2013.08.005.

Cosma, M., Ghinassi, M., D'Alpaos, A., Roner, M., Finotello, A., Tommasini, L., Gatto, R., 2019. Point-bar brink and channel thalweg trajectories depicting interaction between vertical and lateral shifts of microtidal channels in the Venice Lagoon (Italy). Geomorphology 342, 37–50. https://doi.org/10.1016/j.geomorph.2019.06.009.

Costanza, R., Déarge, R., de Groot, R., Farber, S., Grasso, M., Hannon, B., Limburg, K.E., Naeem, S., 1997. The value of the world's ecosystem services and natural capital. Nature 387, 253–260. https://doi.org/10.1038/387253a0.

Da Lio, C., D'Alpaos, A., Marani, M., 2013. The secret gardener: Vegetation and the emergence of biogeomorphic patterns in tidal environments. Philos. Trans. A: Math. Phys. Eng. Sci. 371(2004), 20120367. https://doi.org/10.1098/rsta.2012.0367.

D'Alpaos, A., Lanzoni, S., Marani, M., Rinaldo, A., 2007. Landscape evolution in tidal embayments: Modeling the interplay of erosion, sedimentation, and vegetation dynamics. J. Geophys. Res.: Earth Surf. 112(F1), 1–17. https://doi.org/10.1029/2006JF000537.

D'Alpaos, A., Mudd, S.M., Carniello, L., 2011. Dynamic response of marshes to perturbations in suspended sediment concentrations and rates of relative sea level rise. J. Geophys. Res.: Earth Surf. 116(F4), 1–13. https://doi.org/10.1029/2011JF002093.

D'Alpaos, A., Carniello, L., Rinaldo, A., 2013. Statistical mechanics of wind wave-induced erosion in shallow tidal basins: Inferences from the Venice Lagoon. Geophys. Res. Lett. 40(13), 3402–3407. https://doi.org/10.1002/grl.50666.

D'Alpaos, A., Marani, M., 2016. Reading the signatures of biologic-geomorphic feedbacks in salt-marsh landscapes. Adv. Water Resour. 93, 265–275. https://doi.org/10.1016/j.advwatres.2015.09.004.

D'Alpaos, L., Defina, A., 2007. Mathematical modeling of tidal hydrodynamics in shallow lagoons: A review of open issues and applications to the Venice Lagoon. Comput. Geosci. 33(4), 476–496. https://doi.org/10.1016/j.cageo.2006.07.009.

D'Alpaos, L., 2010. Fatti e misfatti di idraulica lagunare. La laguna di Venezia dalla diversione dei fiumi alle nuove opere delle bocche di porto. Istituto Veneto di Scienze, Lettere ed Arti, Venice (in Italian).

Day, J.W., Britsch, L.D., Hawes, S.R., Shaffer, G.P., Reed, D.J., Cahoon, D.R., 2000. Pattern and process of land loss in the Mississippi Delta: A spatial and temporal analysis of wetland habitat change. Estuaries 23(4), 425–438. https://doi.org/10.2307/1353136.

Day, J.W., Boesch, D.F., Clairain, E.J., Kemp, G.P., Laska, S.B., Mitsch, W.J., Orth, K., Mashriqui, H., Reed, D.J., Shabman, L., et al., 2007. Restoration of the Mississippi Delta: Lessons from hurricanes Katrina and Rita. Science 315(5819), 1679–1684. https://doi.org/10.1126/science.1137030.

Defina, A., 2000. Two-dimensional shallow flow equations for partially dry areas. Water Resour. Res. 36(11), 3251–3264. https://doi.org/10.1029/2000WR900167.

Deheyn, D.D., Shaffer, L.R., 2007. Saving Venice: Engineering and ecology in the Venice Lagoon. Technol. Soc. 29(2), 205–213. https://doi.org/10.1016/j.techsoc.2007.01.014.

Delaune, R.D., Pezeshki, S.R., 2003. The role of soil organic carbon in maintaining surface elevation in rapidly subsiding U.S. Gulf of Mexico coastal marshes. Water Air Soil Pollut. Focus 3, 167–179. https://doi.org/10.1023/A:1022136328105.

Donnelly, J.P., Bertness, M.D., 2001. Rapid shoreward encroachment of salt marsh cordgrass in response to accelerated sea-level rise. Proc. Natl. Acad. Sci. U.S.A. 98(25), 14218–14223. https://doi.org/10.1073/pnas.251209298.

Evans, B.R., Möller, I., Spencer, T., Smith, G., 2019. Dynamics of salt marsh margins are related to their three-dimensional functional form. Earth Surf. Process. Landforms 44(9), 1816–1827. https://doi.org/10.1002/esp.4614.

Feagin, R.A., Barbier, E.B., Koch, E.W., Silliman, B.R., Hacker, S.D., Wolanski, E., Primavera, J.H., Granek, E.F., Polasky, S., Aswani, S., et al., 2008. Vegetation's role in coastal protection. Science 320(5873), 176–177. https://doi.org/10.1126/science.320.5873.176b.

Feagin, R.A., Lozada-Bernard, S.M., Ravens, T.M., Möller, I., Yeager, K.M., Baird, A.H., 2009. Does vegetation prevent wave erosion of salt marsh edges? Proc. Natl. Acad. Sci. U.S.A. 106, 10109–10113. https://doi.org/10.1073/pnas.0901297106.

Ferrarin, C., Tomasin, A., Bajo, M., Petrizzo, A., Umgiesser, G., 2015. Tidal changes in a heavily modified coastal wetland. Continent. Shelf Res. 101, 22–33. https://doi.org/10.1016/j.csr.2015.04.002.

Finotello, A., Lanzoni, S., Ghinassi, M., Marani, M., Rinaldo, A., D'Alpaos, A., 2018. Field migration rates of tidal meanders recapitulate fluvial morphodynamics. Proc. Natl. Acad. Sci. U.S.A. 115(7), 1463–1468. https://doi.org/10.1073/pnas.1711330115.

Finotello, A., Canestrelli, A., Carniello, L., Ghinassi, M., D'Alpaos, A., 2019a. Tidal flow asymmetry and discharge of lateral tributaries drive the evolution of a microtidal meander in the Venice Lagoon (Italy). J. Geophys. Res.: Earth Surf. 124(12), 3043–3066. https://doi.org/10.1029/2019jf005193.

Finotello, A., Lentsch, N., Paola, C., 2019b. Experimental delta evolution in tidal environments: Morphologic response to relative sea-level rise and net deposition. Earth Surf. Process. Landforms 44(10), 2000–2015. https://doi.org/10.1002/esp.4627.

Finotello, A., D'Alpaos, A., Bogoni, M., Ghinassi, M., Lanzoni, S., 2020. Remotely-sensed planform morphologies reveal fluvial and tidal nature of meandering channels. Sci. Rep. 10, 1–13. https://doi.org/10.1038/s41598-019-56992-w.

FitzGerald, D.M., Hughes, Z., 2019. Marsh processes and their response to climate change and sea-level rise. Annu. Rev. Earth Planet Sci. 47, 481–517. https://doi.org/10.1146/annurev-earth-082517-010255.

Gatto, P., Carbognin, L., 1981. The Lagoon of Venice: Natural environmental trend and man-induced modification. Hydrol. Sci. Bull. 26(4), 379–391. https://doi.org/10.1080/02626668109490902.

Gedan, K.B., Silliman, B.R., Bertness, M.D., 2009. Centuries of human-driven change in salt marsh ecosystems. Ann. Rev. Mar. Sci. 1, 117–141. https://doi.org/10.1146/annurev.marine.010908.163930.

Ghinassi, M., D'alpaos, A., Gasparotto, A., Carniello, L., Brivio, L., Finotello, A., Roner, M., Franceschinis, E., Realdon, N., Howes, N., et al., 2018a. Morphodynamic evolution and stratal architecture of translating tidal point bars: Inferences from the northern Venice Lagoon (Italy). Sedimentology 65(4), 1354–1377. https://doi.org/10.1111/sed.12425.

Ghinassi, M., Brivio, L., D'Alpaos, A., Finotello, A., Carniello, L., Marani, M., Cantelli, A., 2018b. Morphodynamic evolution and sedimentology of a microtidal meander bend of the Venice Lagoon (Italy). Mar. Petrol. Geol. 96, 391–404. https://doi.org/10.1016/j.marpetgeo.2018.06.011.

Ghinassi, M., D'Alpaos, A., Tommasini, L., Brivio, L., Finotello, A., Stefani, C., 2019. Tidal currents and wind waves controlling sediment distribution in a subtidal point bar of the Venice Lagoon (Italy). Sedimentology 66(7), 2926–2949. https://doi.org/10.1111/sed.12616.

Howes, N., FitzGerald, D.M., Hughes, Z.J., Georgiou, I.Y., Kulp, M., Miner, M.D., Smith, J.M., Barras, J., 2010. Hurricane-induced failure of low salinity wetlands. Proc. Natl. Acad. Sci. U.S.A. 107(32), 14014–14019. https://doi.org/10.1073/pnas.0914582107.

Hu, Z., van Belzen, J., van der Wal, D., Balke, T., Wang, Z.B., Stive, M., Bouma, T.J., 2015. Windows of opportunity for salt marsh vegetation establishment on bare tidal flats: The importance of temporal and spatial variability in hydrodynamic forcing. J. Geophys. Res.: Biogeosci. 120(7), 1450–1469. https://doi.org/10.1002/2014JG002870.

Kearney, W.S., Fagherazzi, S., 2016. Salt marsh vegetation promotes efficient tidal channel networks. Nat. Commun. 120(7), 1–7. https://doi.org/10.1038/ncomms12287.

Kerr, A.M., Baird, A.H., 2007. Natural barriers to natural disasters. BioScience 57(2), 102–103. https://doi.org/10.1641/b570202.

Kirwan, M.L., Murray, A.B., 2007. A coupled geomorphic and ecological model of tidal marsh evolution. Proc. Natl. Acad. Sci. U.S.A. 104(15), 6118–6122. https://doi.org/10.1073/pnas.0700958104.

Kirwan, M.L., Mudd, S.M., 2012. Response of salt-marsh carbon accumulation to climate change. Nature 489, 550−553. https://doi.org/10.1038/nature11440.

Larsen, L.G., Harvey, J.W., 2010. How vegetation and sediment transport feedbacks drive landscape change in the everglades and wetlands worldwide. Am. Nat. 176(3), 66−79. https://doi.org/10.1086/655215.

Leonardi, N., Fagherazzi, S., 2014. How waves shape salt marshes. Geology 42(10), 887−890. https://doi.org/10.1130/G35751.1.

Leonardi, N., Ganju, N.K., Fagherazzi, S., 2016a. A linear relationship between wave power and erosion determines salt-marsh resilience to violent storms and hurricanes. Proc. Natl. Acad. Sci. U.S.A. 113(1), 64−68. https://doi.org/10.1073/pnas.1510095112.

Leonardi, N., Defne, Z., Ganju, N.K., Fagherazzi, S., 2016b. Salt marsh erosion rates and boundary features in a shallow Bay. J. Geophys. Res.: Earth Surf. 121(10), 1861−1875. https://doi.org/10.1002/2016JF003975.

Luternauer, J.L., Atkins, R.J., Moody, A.I., Williams, H.E., Gibson, J.W., 1995. Salt marshes. Dev. Sedimentol. 53, 307−332. https://doi.org/10.1016/S0070-4571(05)80031-7.

Marani, M., Lanzoni, S., Silvestri, S., Rinaldo, A., 2004. Tidal landforms, patterns of halophytic vegetation and the fate of the Lagoon of Venice. J. Mar. Syst. 51(1−4), 191−210. https://doi.org/10.1016/j.jmarsys.2004.05.012.

Marani, M., Silvestri, S., Belluco, E., Ursino, N., Comerlati, A., Tosatto, O., Putti, M., 2006. Spatial organization and ecohydrological interactions in oxygen-limited vegetation ecosystems. Water Resour. Res. 42(6), W06D06. https://doi.org/10.1029/2005WR004582.

Marani, M., D'Alpaos, A., Lanzoni, S., Carniello, L., Rinaldo, A., 2010. The importance of being coupled: Stable states and catastrophic shifts in tidal biomorphodynamics. J. Geophys. Res.: Earth Surf. 115(F4), F04004. https://doi.org/10.1029/2009JF001600.

Marani, M., D'Alpaos, A., Lanzoni, S., Santalucia, M., 2011. Understanding and predicting wave erosion of marsh edges. Geophys. Res. Lett. 38(21), 1−5. https://doi.org/10.1029/2011GL048995.

Marani, M., da Lio, C., D'Alpaos, A., D'Alpaos, A., 2013. Vegetation engineers marsh morphology through multiple competing stable states. Proc. Natl. Acad. Sci. U.S.A. 110(9), 3259−3263. https://doi.org/10.1073/pnas.1218327110.

Mariotti, G., Fagherazzi, S., Wiberg, P.L., McGlathery, K.J., Carniello, L., Defina, A., 2010. Influence of storm surges and sea level on shallow tidal basin erosive processes. J. Geophys. Res.: Oceans 115(C11), C11012. https://doi.org/10.1029/2009JC005892.

McLoughlin, S.M., Wiberg, P.L., Safak, I., Mcglathery, K.J., 2015. Rates and forcing of marsh edge erosion in a shallow coastal bay. Estuar. Coast 38, 620−638. https://doi.org/10.1007/s12237-014-9841-2.

Mel, R., Carniello, L., D'Alpaos, L., 2019. Addressing the effect of the Mo.S.E. barriers closure on wind setup within the Venice Lagoon. Estuar. Coast. Shelf Sci. 225(30), 104386. https://doi.org/10.1016/j.ecss.2019.106249.

Mion, D., Ghirelli, L., Cazzin, M., Cavalli, I., Scarton, F., 2010. Vegetazione alofila in laguna di Venezia : Dinamiche a breve e medio termine. Lavori Soc. Ven. Sci. Nat. 35, 57−70 (in Italian).

Mitsch, W.J., Gosselink, J.G., 2000. The value of wetlands: Importance of scale and landscape setting. Ecol. Econ. 35(1), 25−33. https://doi.org/10.1016/S0921-8009(00)00165-8.

Möller, I., Spencer, T., French, J.R., Leggett, D.J., Dixon, M., 1999. Wave transformation over salt marshes: A field and numerical modelling study from North Norfolk, England. Estuar. Coast. Shelf Sci. 49(3), 411−426. https://doi.org/10.1006/ecss.1999.0509.

Möller, I., Kudella, M., Rupprecht, F., Spencer, T., Paul, M., van Wesenbeeck, B.K., Wolters, G., Jensen, K., Bouma, T.J., Lange, M.M., et al., 2014. Wave attenuation over coastal salt marshes under storm surge conditions. Nat. Geosci. 7, 727−731. https://doi.org/10.1038/ngeo2251.

Morris, J.T., Sundareshwar, P.V., Nietch, C.T., Kjerfve, B., Cahoon, D.R., 2002. Responses of coastal wetlands to rising sea level. Ecology 83(10), 2869−2877. https://doi.org/10.1890/0012-9658(2002)083[2869:ROCWTR]2.0.CO;2.

Morris, J.T., Barber, D.C., Callaway, J.C., Chambers, R., Hagen, S.C., Hopkinson, C.S., Johnson, B.J., Megonigal, P., Neubauer, S.C., Troxler, T., et al., 2016. Contributions of organic and inorganic matter to sediment volume and accretion in tidal wetlands at steady state. Earth's Future 4(4), 110−121. https://doi.org/10.1002/2015EF000334.

Mudd, S.M., Fagherazzi, S., Morris, J.T., Furbish, D.J., 2004. Flow, sedimentation, and biomass production on a vegetated salt marsh in South Carolina: Toward a predictive model of marsh morphologic and ecologic evolution. In: Fagherazzi, S., Marani, M., Blum, L.K., eds., The Ecogeomorphology of Tidal Marshes, Coastal and Estuarine Studies No. 59. American Geophysical Union, Washington, D.C., pp. 165−188.

Mudd, S.M., D'Alpaos, A., Morris, J.T., 2010. How does vegetation affect sedimentation on tidal marshes? Investigating particle capture and hydrodynamic controls on biologically mediated sedimentation. J. Geophys. Res.: Earth Surf. 115(F3), F03029. https://doi.org/10.1029/2009JF001566.

Mueller, P., Schile-Beers, L.M., Mozdzer, T.J., Chmura, G.L., Dinter, T., Kuzyakov, Y., de Groot, A.V., Esselink, P., Smit, C., D'Alpaos, A., et al., 2018. Global-change effects on early-stage decomposition processes in tidal wetlands: Implications from a global survey using standardized litter. Biogeosciences 15, 3189−3202. https://doi.org/10.5194/bg-15-3189-2018.

Perillo, G.M.E., Wolanski, E., Cahoon, D.R., Brinson, M.M., 2018. Coastal Wetlands: An Integrated Ecosystem Approach. Elsevier.

Priestas, A.M., Fagherazzi, S., 2011. Morphology and hydrodynamics of wave-cut gullies. Geomorphology 131(1−2), 1−13. https://doi.org/10.1016/j.geomorph.2011.04.004.

Pye, K., French, P., 1993. Erosion and Accretion Processes on British Salt Marshes. Cambridge Environmental Research Consultants.

Ratliff, K.M., Braswell, A.E., Marani, M., 2015. Spatial response of coastal marshes to increased atmospheric CO_2. Proc. Natl. Acad. Sci. U.S.A. 112(51), 15580−15584. https://doi.org/10.1073/pnas.1516286112.

Rogers, K., Woodroffe, C.D., 2014. Tidal flats and salt marshes. In: Masselink, G., Gehrels, R., eds., Coastal Environments and Global Change. John Wiley & Sons, Ltd., pp. 227−250.

Roner, M., D'Alpaos, A., Ghinassi, M., Marani, M., Silvestri, S., Franceschinis, E., Realdon, N., 2016. Spatial variation of salt-marsh organic and inorganic deposition and organic carbon accumulation: Inferences from the Venice Lagoon, Italy. Adv. Water Resour. 93, 276−287. https://doi.org/10.1016/j.advwatres.2015.11.011.

Rupprecht, F., Möller, I., Paul, M., Kudella, M., Spencer, T., van Wesenbeeck, B.K., Wolters, G., Jensen, K., Bouma, T.J., Miranda-Lange, M., et al., 2017. Vegetation-wave interactions in salt marshes under storm surge conditions. Ecol. Eng. 100, 301−315. https://doi.org/10.1016/j.ecoleng.2016.12.030.

Sarretta, A., Pillon, S., Molinaroli, E., Guerzoni, S., Fontolan, G., 2010. Sediment budget in the Lagoon of Venice, Italy. Continent. Shelf Res. 30(8), 934−949. https://doi.org/10.1016/j.csr.2009.07.002.

Schoutens, K., Heuner, M., Fuchs, E., Minden, V., Schulte-Ostermann, T., Belliard, J.P., Bouma, T.J., Temmerman, S., 2020. Nature-based shoreline protection by tidal marsh plants depends on trade-offs between avoidance and attenuation of hydrodynamic forces. Estuar. Coast Shelf Sci. 236, 106645. https://doi.org/10.1016/j.ecss.2020.106645.

Schwimmer, R.A., 2001. Rates and processes of marsh shoreline erosion in Rehoboth Bay, Delaware, USA. J. Coast. Res. 17(3), 672−683. https://doi.org/10.2307/4300218.

Shepard, C.C., Crain, C.M., Beck, M.W., 2011. The protective role of coastal marshes: A systematic review and meta-analysis. PLoS ONE 6(11), e27374. https://doi.org/10.1371/journal.pone.0027374.

Signell, R.P., Chiggiato, J., Horstmann, J., Doyle, J.D., Pullen, J., Askari, F., 2010. High-resolution mapping of Bora winds in the northern Adriatic Sea using synthetic aperture radar. J. Geophys. Res.: Oceans 115(C4), 1−20. https://doi.org/10.1029/2009JC005524.

Silvestri, S., Defina, A., Marani, M., 2005. Tidal regime, salinity and salt marsh plant zonation. Estuar. Coast. Shelf Sci. 62(1−2), 119−130. https://doi.org/10.1016/j.ecss.2004.08.010.

Temmerman, S., Bouma, T.J., Govers, G., Wang, Z.B., De Vries, M.B., Herman, P.M.J., 2005. Impact of vegetation on flow routing and sedimentation patterns: Three-dimensional modeling for a tidal marsh. J. Geophys. Res.: Earth Surf. 110(F4), F04019. https://doi.org/10.1029/2005JF000301.

Temmerman, S., Meire, P., Bouma, T.J., Herman, P.M.J., Ysebaert, T., de Vriend, H.J.D., 2013. Ecosystem-based coastal defence in the face of global change. Nature 504, 79–83. https://doi.org/10.1038/nature12859.

Tommasini, L., Carniello, L., Ghinassi, M., Roner, M., D'Alpaos, A., 2019. Changes in the wind-wave field and related salt-marsh lateral erosion: Inferences from the evolution of the Venice Lagoon in the last four centuries. Earth Surf. Process. Landforms 44(8), 1633–1646. https://doi.org/10.1002/esp.4599.

Tonelli, M., Fagherazzi, S., Petti, M., 2010. Modeling wave impact on salt marsh boundaries. J. Geophys. Res.: Oceans 115(C9), C09028. https://doi.org/10.1029/2009JC006026.

Tosi, L., Teatini, P., Brancolini, G., Zecchin, M., Carbognin, L., Affatato, A., Baradello, L., 2012. Three-dimensional analysis of the Plio-Pleistocene seismic sequences in the Venice Lagoon (Italy). J. Geol. Soc. 169(5), 507–510. https://doi.org/10.1144/0016-76492011-093.

van de Vijsel, R.C., Belzen, J., Bouma, T.J., van der Wal, D., Cusseddu, V., Purkis, S.J., Rietkerk, M., van de Koppel, J., 2019. Estuarine biofilm patterns: Modern analogues for Precambrian self-organization. Earth Surf. Process. Landforms 4783. https://doi.org/10.1002/esp.4783.

Wang, H., van der, Wal, D., Li, X.Y., van Belzen, J., Herman, P.M.J., Hu, Z., Ge, Z.M., Zhang, L.Q., Bouma, T.J., 2017. Zooming in and out: Scale dependence of extrinsic and intrinsic factors affecting salt marsh erosion. J. Geophys. Res.: Earth Surf. 122(7), 1455–1470. https://doi.org/10.1002/2016JF004193.

Warren, R.S., Fell, P.E., Rozsa, R., Brawley, A.H., Orsted, A.C., Olson, E.T., Swamy, V., Niering, W.A., 2002. Salt marsh restoration in Connecticut: 20 years of science and management. Restor. Ecol. 10(3), 497–513. https://doi.org/10.1046/j.1526-100X.2002.01031.x.

Xin, P., Zhou, T.Z., Lu, C.H., Shen, C.J., Zhang, C.M., D'Alpaos, A., Li, L., 2017. Combined effects of tides, evaporation and rainfall on the soil conditions in an intertidal creek-marsh system. Adv. Water Resour. 103, 1–15. https://doi.org/10.1016/j.advwatres.2017.02.014.

Young, I.R.R., Verhagen, L.A.A., 1996. The growth of fetch-limited waves in water of finite depth, Part 1: Total energy and peak frequency. Coast. Eng. 29(1–2), 47–78. https://doi.org/10.1016/S0378-3839(96)00006-3.

Yousefi Lalimi, F., Silvestri, S., D'Alpaos, A., Roner, M., Marani, M., 2018. The spatial variability of organic matter and decomposition processes at the marsh scale. J. Geophys. Res.: Biogeosciences 123(12), 3713–3727. https://doi.org/10.1029/2017JG004211.

Zarzuelo, C., D'Alpaos, A., Carniello, L., Ortega-Sánchez, M., Diez-Minguito, M., Finotello, A., Losada, M., 2015. Modeling sand-mud transport in a tidally-dominated bay: Cádiz. In: Proceedings of the XXIV Congress on Differential Equation and Applications, XIV Congress on Applied Mathematics, Càdiz, pp. 1–11.

Zarzuelo, C., López-Ruiz, A., D'Alpaos, A., Carniello, L., Ortega-Sánchez, M., 2018. Assessing the morphodynamic response of human-altered tidal embayments. Geomorphology 320, 127–141. https://doi.org/10.1016/j.geomorph.2018.08.014.

Zecchin, M., Brancolini, G., Tosi, L., Rizzetto, F., Caffau, M., Baradello, L., 2009. Anatomy of the Holocene succession of the southern Venice Lagoon revealed by very high-resolution seismic data. Continent. Shelf Res. 29(10), 1343–1359. https://doi.org/10.1016/j.csr.2009.03.006.

Zhou, Z., Olabarrieta, M., Stefanon, L., D'Alpaos, A., Carniello, L., Coco, G., 2014. A comparative study of physical and numerical modeling of tidal network ontogeny. J. Geophys. Res.: Earth Surf. 119(4), 892–912. https://doi.org/10.1002/2014JF003092.